Estimating Parameters of Subsurface Scattering using Directional Dipole Model

Xingji Zeng, Takafumi Iwaguchi, Hiroyuki Kubo, Takuya Funatomi, Yasuhiro Mukaigawa
Graduate School of Information Science, Nara Institue of Science and Technology
8916-5, Takayama-cho, Ikoma, Nara 630–0192, Japan
{ *zeng.xingji.zq8, iwaguchi.takafumi.il6, hkubo, funatomi, mukaigawa* }*@is.naist.jp*

***Abstract*—Acquisition of parameters for the Bidirectional Scattering Surface Reflectance Distribution Function (BSSRDF) has significant meanings in the study of computer graphics and vision research field. In this paper, we present an inverse rendering approach combined with a newly developed BSSRDF model, directional dipole model, for parameter estimation. To validate our algorithm, we estimate parameters from spheres with a wide range of radius in a simulated and real environment, respectively. According to the observations from both simulated and real experiments, we find that surface curvature significantly affects the estimation results.**

***Keywords*-subsurface scattering, inverse rendering, sphere, computer graphics**

I. Introduction

To synthesize realistic image of translucent material, lots of Bidirectional Scattering Surface Reflectance Distribution Function (BSSRDF) [1], [2], [3] have been proposed to simulate subsurface scattering. Knowing the parameters for these BSSRDF models is not only necessary to render realistic translucent materials, but also have significant meaning in studies of computer vision (CV) like shape acquisition [4].

Parameter acquisition approaches for the BxDF (e.g., BSSRDF) family have appeared in as early as 1999. To estimate parameters of Bidirectional Reflectance Distribution Function (BRDF), inverse global illumination method [5] has been proposed in 1999. Inspired by their work, lots of works to estimate parameters for BSSRDF [1], [6], [2], [7], [4] have been done over the past decades. Whereas, due to the complicated way in which translucent material interacts with light, most previous work is based on the condition of ideally or globally planar surface. Thus, parameter estimation from non-planar surface remains a considerable challenge. As one step towards the solution of inverse rendering problem for an arbitrary non-planar surface, our work focuses on estimating scattering parameters from a spherical surface. Motivated by the theory presented in [8], which shows that the effect of subsurface scattering is strongly correlated to the radius of the sphere, we assume that the radius of sphere also significantly affects the acquisition of parameters from sphere. In this paper, while we do not explicitly give a parameter estimation approach considering the radius of the sphere, we make some progress in this direction by finding a suitable and analytical BSSRDF capable of estimation from a spherical surface and verifying the correlation between sphere curvature and estimation result.

We conclude our work provides a method to estimate BSSRDF parameters from a spherical surface and is a basis for further estimation for an object with complicated shape. Actually, theoretically our mehtod can also be applied to other non-planar surface, but we need more experiments to investigate the accuracy about it.

II. Related work

A. Analytical BSSRDF

To simulate subsurface scattering, conventional path tracing algorithm explicitly traces the transport path of photons inside the material and therefore suffers from the high computational cost. For more practical rendering of translucent material, approximation models for subsurface scattering have been developed to simplify the computation. Early in [1], Jensen et al. introduced a dipole approximation based on diffusion theory. It achieved a plausible trade-off between correctness and efficiency. Though the dipole is limited to the assumption of semi-infinite planar surface and homogeneous material, it is still one of the most widely employed BSSRDF to synthesize translucent material. For the application in more complicated geometries, BSSRDFs are derived from the dipole model, such as multipole [9], [10] for multilayered slab and quadpole [11] for right-angle corner, respectively. In [3], Frisvad et al. introduced a new promotion of the dipole family. On the base of the dipole, the dipole point source was replaced with a set of directional dipole source to meet the boundary condition of the diffusion equation. This new configuration allows their model to formulate the single scattering component into their model. Experiments showed that the directional dipole model can have a closer prediction to the results computed using unbiased path tracing with relatively better efficiency. All these previous works about modeling subsurface scattering offer us a foundation for the analysis of the subsurface scattering.

B. Parameter estimation using inverse rendering

While forming an image from a specified scene is called a rendering process, the techniques used to acquire scene

978-1-5090-5332-2/17 $31.00 © 2017 IEEE
DOI 10.1109/NICOInt.2017.20

information from images are known as inverse rendering. Such kind of techniques for parameter estimation can be traced back to the work of Yu in 1999 [5]. In this work, they first derived a rendering equation for the scene and recovered the surface reflectance and albedo by minimizing the error between observation and simulation. Despite the limitation of opaque material, the basic idea of their work can be seen in later studies. Along with the introduction of the dipole model, Jensen et al. also acquired the parameters for their model by illuminating an optical thick translucent planar surface with collimated beam and searching parameters that best explain the observation in [1]. In [4], Dong et al. simultaneously estimated scattering parameters and surface normal map for globally planar surface by solving a non-liner optimization problem iteratively. To evaluate their estimation of parameters, an approach similar with Jensen et al.[1] was applied as the baseline measurement in their work. Donner et al. specialized the multipole model to better express human skin in [2]. Similarly, they set up a special environment and derived an image formation model for their scene. For the high freedom degree of their model, they chose to solve the optimization problem by utilizing photographs observed under different wavelength. One common ground of these work is that they focus on only a single face of the target sample.

Based on the single scattering approximation, Narasimhan et al. acquired scattering parameters of low concentration participating liquid media using a water tank equipped with a spherical light in [12]. Attributed to their specialized equipment, their work can be applied only to measurement of liquid. Mukaigawa et al. designed an inverse rendering method to acquire the parameters of the dipole model for more complicated shape (e.g., cube, pyramid) in [7]. For more efficient processing, they firstly recovered the diffusion reflectance and then formulate the parameter acquisition as a simple fitting problem. Whereas, a noticeable error between observation and regeneration was presented in their paper. They attributed this error to the over-approximation of the dipole model. This could also be the main motivation for us to choose the directional dipole model [3] instead in our work. Parameter estimation for an object with more complicated shape is also presented. Munoz et al. offered an approach to estimate scattering parameters and reconstruct 3D shape approximately from a single image without any previous knowledge (e.g., shape and light position) in [13]. One limitation of their work is the dependency on being globally convex and optically thick. Gkioulekas et al. challenged the inverse scattering problem of heterogeneous material in [14]. Their method represents 3D volume of smoke using lots of tiny cubes and scattering parameters are estimated for every cube from the input image.

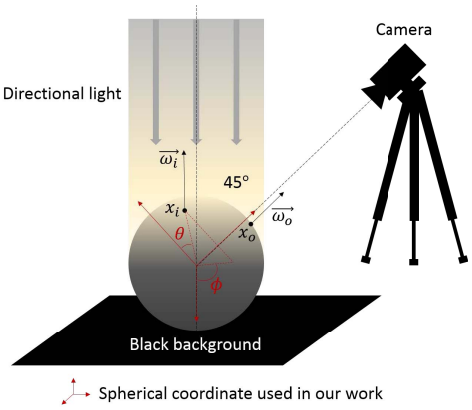

Figure 1: Measurement apparatus

C. Curvature and reflectance

Kolchin et al. presented how surface curvature affects the diffuse reflection of translucent surface by deriving the solution of diffusion equation for a spherical surface in [15]. A noticeable difference was shown between rendering results generated by their proposed solution and by the dipole approximation [1] in their work and it indicates the effect of surface curvature on subsurface scattering. In [8], Kubo et al. developed a Curvature-Dependent Reflectance Function (CRDF) to simulate subsurface scattering more efficiently. They pointed out the fact that the subsurface scattering effect tends to be more noticeable on complex surface and proposed a method to utilize knowledge of curvature to simulate subsurface scattering approximately. Inspired by their work, we are thus interested in inverse rendering approach considering surface curvature.

Compared with the previous works, our work focuses on objects with spherical surface, which would be more complicated than the simply planar surface. While we do not provide a solution to utilize knowledge of surface curvature, a theoretical explanation for the observation is given.

III. Our approach

Like the general inverse rendering method, we design a scene (Fig. 1) and then estimate the parameters for the directional dipole model by optimizing an error function. Different from the previous works, our work focuses on figuring out how the surface curvature affects the accuracy of estimation.

A. Our assumption

As mentioned previously, when ray goes into scattering material, it bounces several times and then goes out from the object. According to the number of bounces, scattering can be literally classified into single scattering and multiple scattering. Imagining a sphere with extremely high curvature, i.e. small radius as shown in Fig. 2, we can intuitively

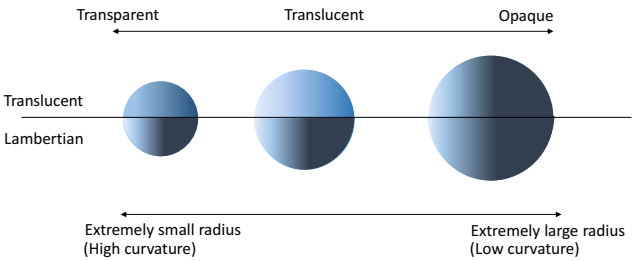

Figure 2: How surface curvature affects translucency

understand that a ray tends to go straight through the sphere. Theregore, single scattering dominates because of the less scattering events. In the opposite case of a sphere with extremely low curvature, i.e. large radius, it is more like a Lambertian surface as the scattering effect is ignorable. According to this intuitive knowledge and theory proposed in [8], we assume that the sphere with a suitable curvature can present more visible translucency effect and offer more details for estimation. In this paper, an inverse rendering method similar with [5][1] is applied for parameter estimation also from a spherical surface. To validate our assumption, we test our fitting approach in simulation and estimate parameters for spheres with different curvatures on real scene.

B. Image formation model

As shown in Fig. 1, a sphere is placed in an ideal dark background so that there is no reflected light from the background. The target sphere is illuminated using a light source with given intensity and position. Instead of the impulse light usually used, a directional light is used for more details of the outgoing radiance change. Photographs are taken from 45 degrees away from the surface normal direction. The outgoing radiance $L_o(x_o, \vec{\omega}_o)$ is in accordance with the following integral.

$$L_o(x_o, \vec{\omega}_o) = \int_A \int_{2\pi} S(x_i, \vec{\omega}_i; x_o, \vec{\omega}_o) L_i(x_i, \vec{\omega}_i)(n_i \cdot \omega_i) d\omega_i dx_i, \quad (1)$$

where A is the surface area of sphere. With a directional light source, we can simplify Eq. (1) to an simpler integral only on the surface area:

$$L_o(x_o, \vec{\omega}_o) = \int_A S(x_i, \vec{\omega}_i; x_o, \vec{\omega}_o) L_i(x_i, \vec{\omega}_i)(n_i \cdot \omega_i) dx_i, \quad (2)$$

where ω_i becomes a constant vector as shown in Fig. 1. As mentioned above, single scattering becomes significant in the case of high curvature. Conventionally, most of BSSRDF approximations can only formulate multiple scattering and single scattering is processed by an additional ray tracer. In our work, the directional dipole model is chosen for prediction. As Frisvad et al. formulate the single scattering in their BSSRDF approximation [3], we can thus cover single scattering with reasonable time consuming by applying their model. The full BSSRDF with the directional dipole approximation is

$$S = T_{12}(S_d + S_{\delta_E})T_{21}, \quad (3)$$

where T_{12} and T_{21} are the Fresnel transmittance terms at point x_i and x_o, respectively. S_{δ_E} models single scattering along the refracted direction. S_d models single scattering from other direction and multiple scattering components and is a function of parameters shown in Table I. For explicit definition of S_d and S_{δ_E} can be found in [3]. As there is no refracted light in our scene, we simplify Eq. (3) to $S = T_{12}S_dT_{21}$. Combining Eq. (2) and Eq. (3), we get the following equation.

$$L_o(x_o, \vec{\omega}_o) = \int_A T_{12} S_d(x_i, \vec{\omega}_i; x_o, \vec{\omega}_o) L_i(x_i, \vec{\omega}_i)(n_i \cdot \omega_i) T_{21} dx_i \quad (4)$$

With Eq. (4), we now can simulate the observation given appropriate parameters for the directional dipole model.

Table I: Parameters for the directional dipole model

σ_a	absorption coefficient
σ_s	scattering coefficient
g	mean cosine of the scattering angle
η	relative index of refraction

C. Optimization problem

Like previous methods, parameters can be estimated for each color channel respectively using our approach. In this paper, only parmeters of red channel are estimated. When we acquire an observed image of the scene, instead of rendering the whole scene, we extract an 1D slice from the red channel of the observed image and make a graph as shown in Fig. 6 for estimation. The x-axis of the graph is the polar angle of x_o (Fig. 1). Y-axis of the graph are the pixel value of observation and can be computed with Eq. (4). As mentioned previously, to compute S_d, theoretically four unknown parameters shown in Table I are needed to be estimated. As there is already established technique to measure index of refraction for objects, we decide to lay more emphasis on estimation of scattering parameters and use the reference value of different material for our estimation. By accepting the assumption of isotropic scattering in our case, we can further set $g = 0$.

Now we can estimate the remained parameters by optimizing the error between the observation and the prediction.

$$(\sigma_a, \sigma_s) = \arg\min_{\sigma_a, \sigma_s} \sum_{k=0}^{N} (L_{obs}(p_k) - L_{pdt}(p_k))^2, \quad (5)$$

in which p_k is the position of the image pixel of x_o in the 3D scene, and N is the total number of pixels in the image.

Table II: Results of different sphere in simulation

Parameter	$\sigma_a(mm^{-1})$	$\sigma_s(mm^{-1})$
Ground truth	0.0010	0.1000
Estimation	0.0010	0.1000
Ground truth	0.1000	0.0010
Estimation	0.1000	0.0010

$L_{obs}(p_k)$ and $L_{pdt}(p_k)$ mean the radiance at corresponding point x_o, which are given by observation and Eq. (4) respectively. According to Eq. (5), we set up experiments on simulation and real scene.

IV. Experiment on simulation scene

To validate our fitting approach, we firstly estimate the parameters from simulation data such that the influences from real scene can be avoided. Benefiting from the high resolution of recent DSLR cameras, which is supposed as 6000×4000 in this experiment, we get a good observation of the sphere even though the camera is far away from the sphere. And the useful region in the image was only approximately 500×500. To reduce the processing time, we render the useful region in the image directly. As the camera is far away enough, it can be approximated to an orthographic projection. We thus implement an orthographic camera in all of our image formation process for simplicity. Input data is generated using the directional dipole model. We extract a 1D slice from the generated data as input and do a optimization according to Eq. (5) using direction dipole model. Estimation result is shown in Table II. Since same model is used in both data generation and optimization, a good result is acquired.

According to the fitting result, the parameters were estimated exactly from the spherical surface, which means our fitting approach is reliable.

V. Experiment on real scene

A. Setup of environment

We test the robustness of our algorithm by estimating the parameters from observed data acquired from a real environment. To interpret our scene, we use an Optoma ML750 LED projector as our light source. We create a directional light by placing the projector far away enough and project a circle pattern onto the sphere. A Nikon D5300 is used for observation. To take the photograph from 45 degree as shown in Fig. 1, we do a alignment shown in Fig. 4b. By overlapping $line\ a$ and $line\ b$, the observation angle of camera can be set to 45 degree to the light direction. With a LED projector, background region that should be black is also illuminated as the projector cannot really project a dark light. To eliminate the noise of the stray light, we subtract a dark image, taken with projecting a black image to the scene, from each measurement and reference. To avoid reflected light from the background, we adjust the size of the projected pattern to be the same as the size of the sphere. In the experiment on the real scene, we cannot set the radiance of the light source like the one in simulation. Another difficulty is that the result is affected by the optical property of the camera lens and CCD, which would be unknown to us. Mathematically, we can modify equation 4 to

$$I_o(x_o, \vec{\omega}_o) = K \int_A T_{12} S_d(x_i, \vec{\omega}_i; x_o, \vec{\omega}_o) L_i(x_i, \vec{\omega}_i)(n_i \cdot \omega_i) T_{21} dx_i, \tag{6}$$

where $I_o(x_o, \vec{\omega}_o)$ is the pixel value at the point x_o viewed from the direction ω_o and K is the camera sensor response. As mention above, $L_i(x_i, \vec{\omega}_i)$ and K is unknown in Eq. (6). To solve these problems, we take the reference image of Labsphere Spectralon, $reflectance > 0.99$, as an ideal white diffuser reflector. According to the Lambert property of the ideal diffuser, diffusive reflectance of the diffuser is $R_{diffuser} = \frac{1}{\pi}$. We place the diffuser at the same place as the sphere and illuminate it with the same pattern used for the sphere. The pixel value of the diffuser is formulated as following:

$$I_{diffuser}(x'_i) = K L_o(x'_i, \vec{\omega}'_i)(\vec{n}'_i \cdot \vec{\omega}'_i) R_{diffuser}, \tag{7}$$

where $I_{diffuser}(x'_i)$ is the pixel value of point x'_i on the diffuser. Based on the condition of directional light, intensity of radiance is a constant independent from the position x'_i. Therefore, we have $L_i(x_i, \vec{\omega}_i) = \overline{L}$ and $I_{diffuser}(x'_i) = \overline{I}_{diffuser}$, which mean that incoming radiance and observed pixel value are identical to the mean of all points. We then reshape Eq. (7) to $K\overline{L} = \frac{\overline{I}_{diffuser}}{(\vec{n}'_i \cdot \vec{\omega}'_i)}$. In other words, $K\overline{L}$, which is needed in equation 6, can be acquired together by Eq. (7). For simplicity, we make the direction of the directional light perpendicular to the diffuser surface so that we have $\vec{n}'_i \cdot \omega'_i = 1$. To configure the scene exactly, we also make some alignment to the measure tools. To ensure the direction of light source is perpendicular to the diffuser surface, we project a slim ray to the mirror so that there would be a reflected ray on the lens of the projector. Note that the surface of the mirror is parallel to the one of the diffuser. By overlapping the reflected point on the emitting point, we can make sure the direction of light source is perpendicular to the mirror and also to the diffuser. To illuminate the diffuser, we still need to replace the mirror with the diffuser. To do this, we fix the mirror and the diffuser on a stage that can move horizontally. Once the light direction is set, we can simply move the diffuser to the position of the mirror while preserving their parallelism. To eliminate the effect of specular reflection, we use a pair of cross-polarization to filter out the glossy surface reflection. However, doing this also brings a side effect that also eliminates the single scattering events, which will be discussed in details in following section. To generate the scattering profile, we also need to know the x-axis, the polar angle (θ) of point x_i when the sphere is placed in

the spherical coordinate system. This can be computed by the following equation.

$$\theta = \frac{\pi}{2} - \arcsin\left(\frac{y_w}{R}\right), \tag{8}$$

where y_w is the y coordinate in the world coordinate and R is the radius of the sphere. y_w can be acquired by transforming the UV coordinates of specified pixel p_k to the world coordinate of the corresponding point x_o(Fig. 3) using the following equation:

$$(x_w, y_w) = ((\frac{Width}{2} - (0.5+u))dx, (\frac{Height}{2} - (0.5+v))dy) \tag{9}$$

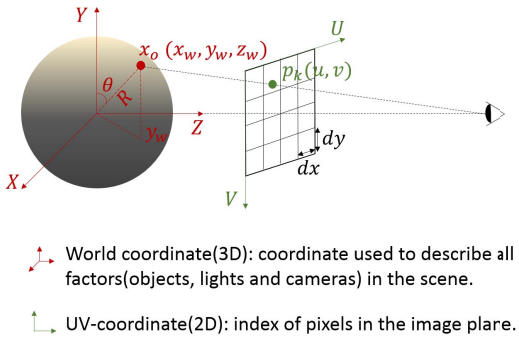

Figure 3: Transformation from world coordinate to UV coordinate

where $dx = \frac{2R}{Width_{img}}$ and $dy = \frac{2R}{Height_{img}}$, which mean the length in the real world per pixel in horizontal and vertical directions. $Width_{img}$ and $Height_{img}$ mean the resolution of image in horizontal and vertical direction. For comparison, we prepare three different nylon spheres as our target.

B. Results and conclusion

As shown in Fig. 6, fitting result of directional dipole model get worse in sphere with radius $R = 6.36$mm. Different from experiment on simulation scene, we do not know the ground truth of the parameters. To evaluate the estimation results in Table III, we render the spheres using estimated parameters for each sphere correspondingly and compare the error between observation and prediction of different spheres. As outgoing radiance $L_o(x_o, \vec{\omega}_o)$ in smaller sphere tends to be smaller and therefore it have a smaller error despite its worse fitting, the sum of absolute error may not be able to equally evaluate the estimation of different spheres. For justifying the evaluation, we use the following error instead:

$$E' = \frac{1}{N}\sum_{k=0}^{N}\frac{\|L_{obs}(p_k) - L_{pdt}(p_k)\|}{L_{obs_{\max}}}. \tag{10}$$

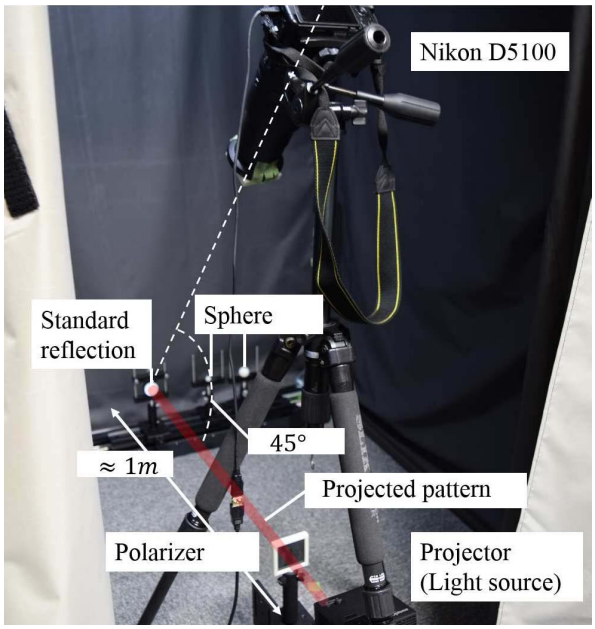

(a) Environmental setup

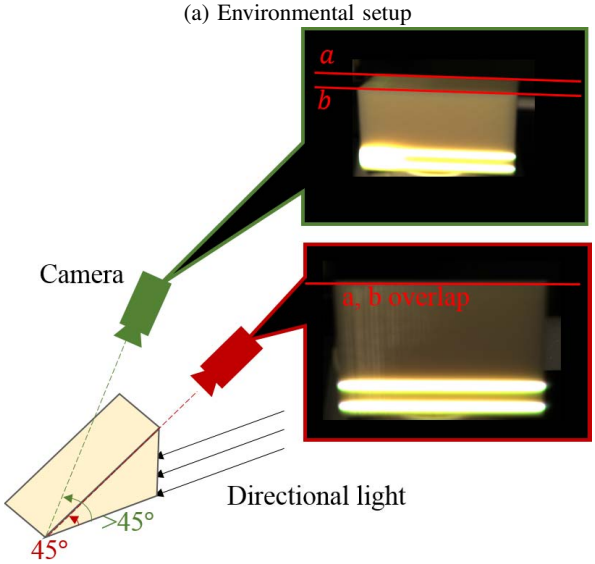

line a and line b overlap when camera views from 45 degree.

(b) Alignment for view direction

Figure 4: Experimental environment

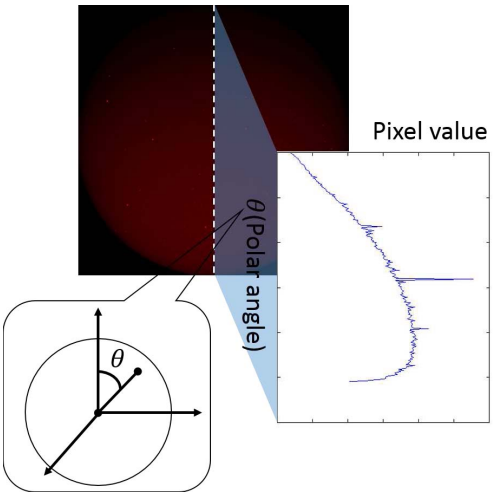

Figure 5: Input of estimation alogorithm

Table III: Results of different sphere in real scene

Directional dipole model			
Radius(mm)	6.36	9.55	12.72
σ_a	0.0000	0.0046	0.0025
σ_s	0.3600	0.4428	0.3549
E'	0.1421	0.1338	0.1857

Dipole model			
Radius(mm)	6.36	9.55	12.72
σ_a	0.0390	0.0417	0.0625
σ_s	0.0551	0.0861	0.0801
E'	0.5014	0.2013	0.2904

According to Fig. 7, almost same level of error are observed despite of the different radius of spheres. Since the available samples are limited, experiment for more spheres could not have done in our work. We attribute this observation to the reason that the spheres are not small or big enough to lose the translucent effect.

We also make the comparison with dipole in our experiment on real scene (Fig. 6 and Table III). Estimation error of the dipole model grows acutely in the case that $R = 6.36$mm. The directional dipole model also presents more stable result than the original dipole model. However, it still shows a better estimation at the middle range of the curvature, which also meets our expectation. In a whole, estimation using directional dipole model shows lower error. Given all of these experiment results, we validate our assumption that the curvature of the sphere affects the estimation results and verify the good performance of the directional dipole model in parameter estimation. We can make a further assumption that accuracy of the conventional inverse rendering method for parameter estimation can be improved by well utilizing the preliminary of the surface curvature.

VI. Discussion

A. Specular reflection

Originally, we select the directional dipole model for our estimation because of its capability of covering single scattering. Nevertheless, we use a pair of cross-polarization to filter out specular reflection, which meanwhile eliminates the single scattering events. Despite this, we still have better result in the directional dipole model than the original dipole model. We attribute this to the possibility that the directional dipole model can also model multiple scattering better than the original dipole model.

B. Assumption of Directional Dipole Model

Same as the dipole model, the directional dipole model solves the diffuse function on a semi-infinite planar surface. That is, strictly, directional dipole is theoretically correct only on semi-infinite planar surface. When the directional dipole model is used for non-planar surface, it becomes inaccurate, though, it still has a better performance than the dipole model. Referring to the results shown in [3], we believe that the directional dipole model is the most robust to surface shape by now.

C. Preliminary of shape

Similarly to most of the previous inverse rendering methods, one limitation of our method is the dependency on given shape. Because of the ambiguity between the shape and the subsurface scattering parameters, simultaneous estimation of shape and parameters would be a challenging task. Iterative approach like the work in [4] may be a interesting direction for solving this problem.

D. Slow processing

In our work, it takes hours to finish one estimation. We attribute this low efficiency to the high computational cost of the path tracing. For each x_o in Eq. (4), we run a Monte Carlo approach with uniform sampling to compute the integral over the surface. We know that implementing more effective sampling approach, e.g. importance sampling, helps to solve the problem, though, we choose not to do this in our work.

VII. Conclusion and Future Work

In this paper, we propose an inverse rendering method for estimating scattering parameters from spherical surface. Different from the previous work, we pay attention to a factor, surface curvature, which is generally ignored. We make an assumption that surface curvature affects the estimation result and design some experiments on simulation and real scene to validate our approach. To better do the parameter estimation on spherical surface, we also choose the directional dipole model newly introduced in [3] as our prediction model. Experimental results show that as surface curvature changes from extremely low to extremely

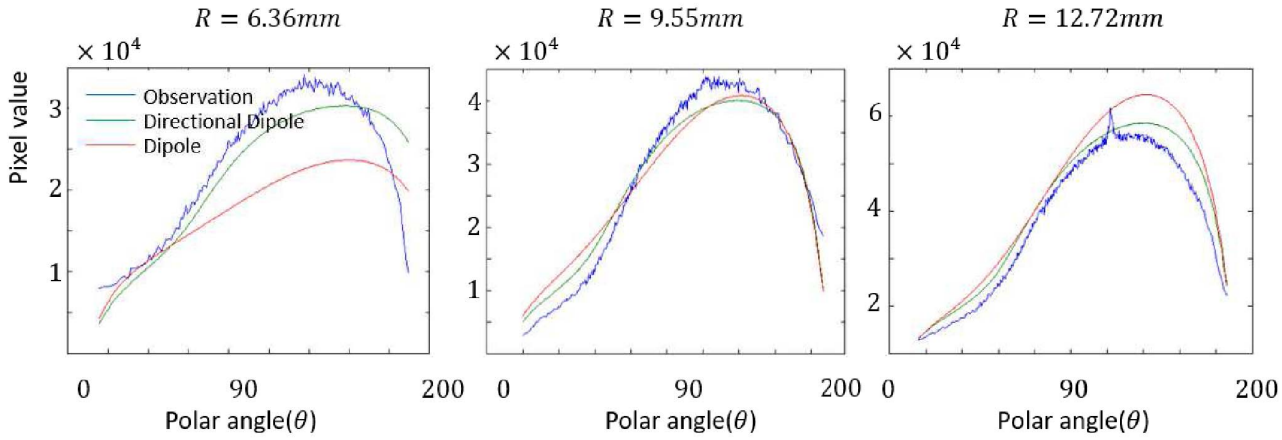

Figure 6: Fitting results of estimation

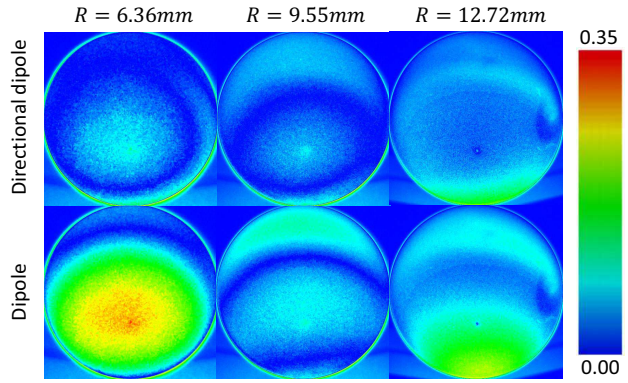

Figure 7: Reproduction compared with real observation

high, there exists a range of curvature that minimizes the estimation error. We can thus further say that we can improve the estimation quality by choosing a most suitable curvature for the estimation. By comparing the estimation result of the directional dipole model and the original dipole model, we also validate our choice of the directional dipole model. In future work, we plan to apply our assumption to estimation of surface with changing curvature, instead of surface with constant curvature like a sphere. We expect to achieve a better estimation by choose the suitable data in the image according to the surface curvature. Based on the assumption that our target object optically thick, mean cosine of the scattering angle g is set 0, though, in case of high curvature this assumption may be broken. Therefore future research about simultaneous estimation including other sacttering parameters will also be a interesting direction.

Acknowledgements

The authors would like to thank Jeppe Revall Frisviad for answering our questions about the directional dipole model.

This work was supported by JSPS KAKENHI Grant Number JP15K16027.

References

[1] H. W. Jensen, S. R. Marschner, M. Levoy, and P. Hanrahan, "A practical hogehoge model for subsurface light transport," in *Proceedings of the 28th Annual Conference on Computer Graphics and Interactive Techniques*, ser. SIGGRAPH '01. New York, NY, USA: ACM, 2001, pp. 511–518. [Online]. Available: http://doi.acm.org/10.1145/383259.383319

[2] C. Donner, T. Weyrich, E. d'Eon, R. Ramamoorthi, and S. Rusinkiewicz, "A layered, heterogeneous reflectance model for acquiring and rendering human skin," in *ACM SIGGRAPH Asia 2008 Papers*, ser. SIGGRAPH Asia '08. New York, NY, USA: ACM, 2008, pp. 140:1–140:12. [Online]. Available: http://doi.acm.org/10.1145/1457515.1409093

[3] J. R. Frisvad, T. Hachisuka, and T. K. Kjeldsen, "Directional dipole model for subsurface scattering," *ACM Trans. Graph.*, vol. 34, no. 1, pp. 5:1–5:12, Dec. 2014. [Online]. Available: http://doi.acm.org/10.1145/2682629

[4] B. Dong, K. D. Moore, W. Zhang, and P. Peers, "Scattering parameters and surface normals from homogeneous translucent materials using photometric stereo," in *IEEE International Conference on Computer Vision and Pattern Recognition*, June 2014, pp. 2299–2306.

[5] Y. Yu, P. Debevec, J. Malik, and T. Hawkins, "Inverse global illumination: Recovering reflectance models of real scenes from photographs," in *Proceedings of the 26th Annual Conference on Computer Graphics and Interactive Techniques*, ser. SIGGRAPH '99. New York, NY, USA: ACM Press/Addison-Wesley Publishing Co., 1999, pp. 215–224. [Online]. Available: http://dx.doi.org/10.1145/311535.311559

[6] S. G. Narasimhan, M. Gupta, C. Donner, R. Ramamoorthi, S. K. Nayar, and H. W. Jensen, "Acquiring scattering properties of participating media by dilution," *ACM Transactions on Graphics*, vol. 25, p. 1003, 2006.

[7] Y. Mukaigawa, K. Suzuki, and Y. Yagi, "Analysis of subsurface scattering based on dipole approximation," *IPSJ Transactions on Computer Vision and Applications*, vol. 1, pp. 128–138, 2009.

[8] H. Kubo, Y. Dobashi, and S. Morishima, "Curvature-dependent reflectance function for interactive rendering of subsurface scattering." *International Journal of Virtual Reality*, vol. 10, no. 1, 2011.

[9] C. Donner and H. W. Jensen, "Light diffusion in multi-layered translucent materials," *ACM Trans. Graph.*, vol. 24, no. 3, pp. 1032–1039, Jul. 2005. [Online]. Available: http://doi.acm.org/10.1145/1073204.1073308

[10] C. Donner and H. W. Jensen, "Rapid simulation of steady-state spatially resolved reflectance and transmittance profiles of multilayered turbid materials," *J. Opt. Soc. Am. A*, vol. 23, no. 6, pp. 1382–1390, Jun 2006. [Online]. Available: http://josaa.osa.org/abstract.cfm?URI=josaa-23-6-1382

[11] C. Donner and H. W. Jensen, "Rendering translucent materials using photon diffusion," in *ACM SIGGRAPH 2008 Classes*, ser. SIGGRAPH '08. New York, NY, USA: ACM, 2008, pp. 4:1–4:9. [Online]. Available: http://doi.acm.org/10.1145/1401132.1401138

[12] S. G. Narasimhan, M. Gupta, C. Donner, R. Ramamoorthi, S. K. Nayar, and H. W. Jensen, "Acquiring scattering properties of participating media by dilution," in *ACM SIGGRAPH 2006 Papers*, ser. SIGGRAPH '06. New York, NY, USA: ACM, 2006, pp. 1003–1012. [Online]. Available: http://doi.acm.org/10.1145/1179352.1141986

[13] A. Munoz, J. I. Echevarria, F. J. Seron, J. Lopez-Moreno, M. Glencross, and D. Gutierrez, "Bssrdf estimation from single images," in *Computer Graphics Forum*, vol. 30, no. 2. Wiley Online Library, 2011, pp. 455–464.

[14] I. Gkioulekas, A. Levin, and T. Zickler, "An evaluation of computational imaging techniques for heterogeneous inverse scattering," in *European Conference on Computer Vision*. Springer, 2016, pp. 685–701.

[15] K. Kolchin, "Surface curvature effects on reflectance from translucent materials," *CoRR*, vol. abs/1010.2623, 2010. [Online]. Available: http://arxiv.org/abs/1010.2623